A Technique for Obtaining Shock-Wave Parameters Using Wave Superposition in Low-Carbon Steel

MARC A. MEYERS, CARLOS SARZETO, AND CHEN-YIH HSU

A novel experimental set-up for obtaining shock-wave superposition is described. Detonation is simultaneously initiated at the two opposite sides of an explosive layer placed directly in contact with a steel block. It was possible to take advantage of the α (bcc) $\rightarrow \epsilon$ (hcp) $\rightarrow \alpha$ (bcc) transformation occurring in iron at approximately 13 GPa in a unique fashion. The pressure of the two converging pulses is approximately 13 GPa, resulting in little or no transformation. However, in the region of superposition of the two waves the pressure is much higher. *Post explosionem* observation of the microstructure allowed an easy identification of the region of superposition, because of the profuse transformation "debris". Events conducted for three thicknesses of the explosive layers allowed conclusions to be drawn about the changes of rarefaction and attenuation rates. The interactions occurring between the waves due to simultaneous superposition and transformation are thought to be responsible for internal spalling.

1. INTRODUCTION

THE parameters that affect the shock-loading response of metals may be divided into two categories: a) material parameters, such as the composition of the alloy, grain size, preshock history, temperature prior to shocking; and b) shock-wave parameters, such as peak pressure, pulse duration, attenuation rate, internal reflections. In the majority of the investigations conducted to study the effects of aforementioned parameters, the experimental set-up used to generate the shock wave consists of a driver plate (accelerated by explosives or other means) impacting the system. This set-up yields a finite pulse duration, determined by the driver-plate thickness. The pressure and rarefaction rate are dictated by the driver-plate velocity and material, respectively. On the other hand, set-ups where the explosive is in direct contact with the work-piece yield a zero pulse duration and a pressure and rarefaction rate dictated by the characteristics of the explosive and the angle between the detonation front and the explosive-workpiece interface.

In this investigation, an attempt was made to understand the mechanisms of propagation of waves generated by contact explosives in low-carbon steel. It was possible to take advantage of the α (bcc) $\rightarrow \epsilon$ (hcp) $\rightarrow \alpha$ (bcc) transformation occurring in iron (*e.g.*, Ref. 1) in a unique fashion. The single shock wave generated pressures of around 13 GPa, with $\alpha \rightarrow \epsilon \rightarrow \alpha$ transformation restricted to the surface of the blocks. However, in the region where shock-wave superposition occurred, the pressure rose above this value, inducing the transformation, whose "debris" are easily seen in the residual microstructure. Internal markers generated by the transformation allow conclusions about the nature of the shock wave. Additionally, internal spalling generated by shock-wave superposition was detected.

2. EXPERIMENTAL TECHNIQUES

Figure 1 shows the experimental set-up used in the investigation. A detonator having its extremity imbedded in the primary booster charge transmits the detonation to the center of a segment of Primacord, so that the explosive front reaches the two secondary boosters simultaneously. The secondary boosters were fabricated in such a way that the extremity of the Primacord was perpendicular to the plane of the line-wave generator. Preliminary experiments laying the Primacord on top of the tip of the line-wave generator and covering it with supplementary layers of explosive were not successful. The failure is thought to be due to jetting that occurs at the extremity of the Primacord. Line-wave generators transmit the detonation to the main charge, that consists of layers of Plastex-P in intimate contact with the upper surface of a steel block. The boosters and line-wave generators were also fabricated with Plastex-P. The line-wave generator was fabricated by inserting a Plastex-P sheet between two triangular dies of stainless steel sheet in which the appropriate hole pattern had been drilled; the holes were made by inserting a steel punch in all orifices. Plastex-P is a PETN-base, laminated (2 mm sheets) explosive fabricated in Brazil; its characteristics closely resemble those of Detasheet C and will be assumed to be the same, in the calculations that follow. The objective of this set-up was to assure the encounter of the two wave fronts at approximately the center of the steel block. Three explosive events were conducted,

MARC A. MEYERS and CHEN-YIH HSU, formerly with the Department of Metallurgical Engineering, South Dakota School of Mines and Technology, are presently Associate Professor and Graduate Research Assistant, Department of Metallurgical and Materials Engineering, New Mexico Institute of Mining and Technology, Socorro, NM; CARLOS SARZETO is Major, Brazilian Army, and Professor, Secao de Mecanica, Instituto Militar de Engenharia, Rio de Janeiro, Brasil.

Manuscript submitted October 9, 1979.

ISSN 0360-2133/80/1013-1737$00.75/0

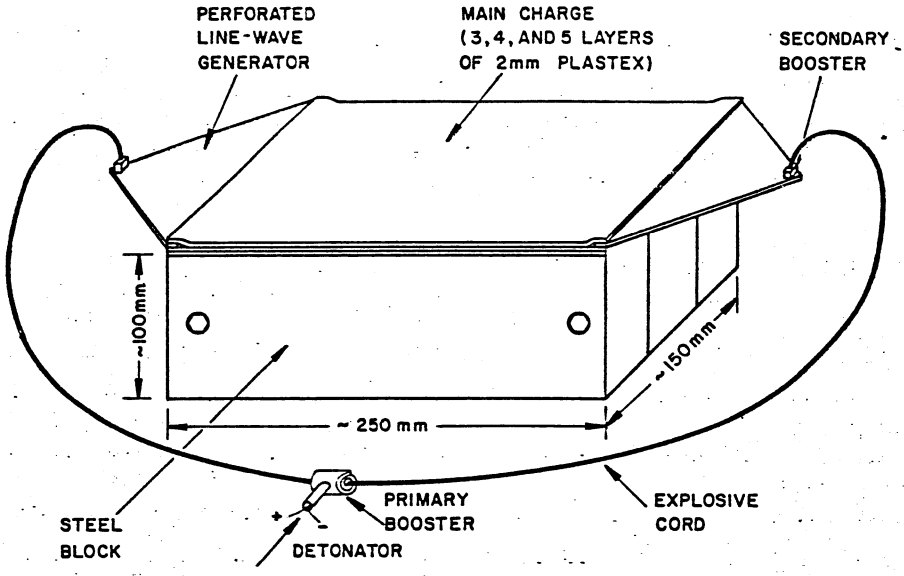

Fig. 1—System used to obtain shock-wave superposition (lateral momentum traps not shown).

using three, four and five layers of Plastex-P as the main charge.

The steel block was made from 4 in. (10.2 cm) thick, hot-rolled AISI 1020 steel. It was sliced into two or three plates; the internal faces were planer milled; the sections were bolted together, as indicated in Fig. 1. The external sides of the whole assembly were then planer milled. The objective of the sectioning was to provide an easier *post explosionem* observation. The whole assembly was placed on top of a massive steel block which absorbed all waves directly impinging on the lower surface of the block. The blocks were surrounded on the four sides by momentum traps whose objective was to absorb the reflecting waves.

The steel blocks were annealed at 950 K for 2 h in a controlled atmosphere. This heat treatment yielded grain sizes of 58, 50 and 48 μm determined by the linear intercept method, for the blocks shocked with three, four and five layers of Plastex-P, respectively.

For optical microscopy, the steel was etched with 2 pct Nital. For the macrographs, Fry's reagent was used. The observation of the fractures was carried out in a Coates and Welter scanning electron microscope.

3. CALCULATION OF SHOCK-WAVE PARAMETERS

The shock waves generated by explosives directly in contact with the workpiece are characterized by a peak-pressure pulse duration equal to zero. This type of wave is called "saw-tooth shaped" by Rinehart[2]. The peak pressure for normal shock-wave incidence in direct contact explosives can be determined by the impedance matching technique. The transmission pressure *vs* particle-velocity curve has to be matched with the reflection curve of the explosives. The procedure is described by Duvall and Fowles, [3] Jones,[4] and Orava and Wittman.[5] The pressure *vs* particle-velocity curves for the explosives pass through the Chapman-Jouguet state. Since the pressure *vs* particle-velocity curves for Detasheet C and its Brazilian equivalent Plastex-P are not given by Duvall and Flowles[3] or Jones,[4] Orava and Wittman[5] calculated the Chapman-Jouguet pressure and particle velocity and passed the curve through this point. It is acceptable to obtain the curve from a single point because the curves for all other explosives closely resemble each other and are "parallel". This is shown in Fig. 2. The Detasheet C curve intersects the iron curve at a pressure of 32 GPa; this is the pressure generated in iron by normally incident shock waves. Since the detonation front propagates parallel to the surface, one has to introduce a correction. The results of Jones[4] for iron and Composition B indicate that a multiplying factor of 0.412 provides the correct pressure. Applying this factor one obtains a pressure of 13.2 GPa. It will be seen in Section 4 that this calculation is correct. Since the pressure in contact operations is not a function of the thickness of the explosive layer, it should be the same for the three systems. The pulse duration at the peak pressure is zero.

The angle between the shock front and the top surface of the block at the interface (see Fig. 3(*a*)), can

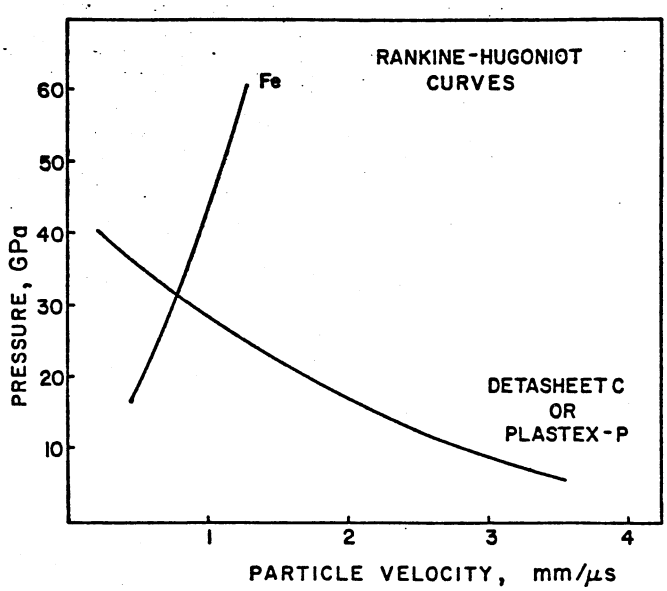

Fig. 2—Rankine-Hugoniot curves for iron and Plastex-P. For iron, the transmitted curve is used; for the explosive, one uses the reflected curve.

be calculated by applying Equation 1 of Katz *et al.*[6]

$$\sin \alpha = \frac{U_s}{U_d}$$

where U_s is the velocity of the shock wave and U_d is the velocity of detonation of the explosive. U_d is equal to 6,800 m/s for Detasheet C. Barker[7] made a careful analysis the velocity U_s as a function of pressure and found it to be linearly related to the particle velocity, U_p:

$$U_s = C_o + 1.33\, U_p$$

where C_o is the velocity of elastic dilational waves (C_o = 4.63 mm/μs). It is instructive to compute the angle α for three values of the pressure. From the Hugoniot pressure *vs* particle velocity plot, one obtains values of 0, 0.21, and 0.395 mm/μs for pressures of 0, 6.5, and 13 GPa. This, in turn, yields angles α:

$$\alpha_{0\,GPa} = 42.9 \text{ deg}$$

$$\alpha_{6.5\,GPa} = 46.2 \text{ deg}$$

$$\alpha_{13\,GPa} = 49.4 \text{ deg}$$

Hence, there is some degree of curvature in the shock-wave fronts. The angle decreases from 49.4 deg, at the top surface, to 42.9 deg, at the extreme bottom of the wave. This curvature will be discussed in Section 4.

The rarefaction rates were not calculated because the mathematical procedures are very complex, involving the characteristic curves and the method of finite differences.[8-10]

4. EXPERIMENTAL RESULTS

4.1 Shock-wave Superposition

Figure 3(*a*) shows schematically the shock-wave configuration created by the detonation fronts. For simplicity, the shock fronts are assumed to be straight. The pressure attenuates as the front penetrates into the material. Therefore, the wave is represented by isobaric lines in Fig. 3(*a*). It is assumed that the rarefaction rate is contant; this is indicated by the equidistant isobaric lines. When the two wave fronts encounter each other, the resulting pressure at a certain point is assumed to be the sum of the pressures due to the two waves. Strictly speaking, the pressures are not exactly additive because a) the pressure *vs* compressibility curve is not exactly linear and b) the phase transformation occurring at 13 GPa promotes a partial collapse of the lattice. However, up to the level of 13 GPa total pressure (from the two waves) these effects are not of great importance. Hence, in the particular configuration shown in Fig. 3(*b*) the pressures were simply added; the circled numbers are the total pressures. The isobaric lines were traced for pressures at 2 GPa intervals. At a distance D from the surface the pressure rises to 14 GPa, while the pressure generated by the individual waves is 7 GPa. The 14 GPa pressure is enough to effect the α (bcc) $\rightarrow \epsilon$ (hcp) transformation.

Figure 4(*a*) shows an internal face of the block subjected to an explosion with three Plastex-P layers. The block was etched with Fry's reagent. The dark region is the material in which the pressure was sufficiently high to produce the α (bcc) $\rightarrow \epsilon$ (HCP) transformation. The section of the transmation region is approximately triangular. Figure 4(*b*) shows the transformation regions for the three systems. These sections correspond to portions cut from the central regions of the blocks. Longitudinal cuts had to be made in the blocks because the shock wave interacted with the internal surface. The blocks subjected to four and five layers of Plastex-P fractured after the passage of the waves because the momentum traps were not completely effective in stopping the reflected waves. The width and depth of the transformation regions are given in Table I; the width is heavily dependent upon the thickness of the explosive layer, while the depth is much less affected.

The hardness results are consistent with the macrograph results. Figure 5(*a*) shows the hardness profiles at the surface of the block subjected to three explosive layers and at depths of 3.8, 30, and 60 mm below the surface. The surface exhibits a hardness of approximately R_A60 throughout the overall length. At 3.8 mm below the surface the hardness drops to R_A45. The dots in the plot are individual hardness measurements; they were connected by segments, and the apparent width of the interaction regions, as seen by the hardness measurements, is larger than the true width. The abrupt hardness increase when the pressure of 13 GPa is exceeded is well documented in the literature[11-13]. After 3.8 mm below the surface, the hardness decrease is more gradual. Figures 5(*b*) and (*c*) show hardness profiles along lines perpendicular to the top surface of the blocks at two positions: the wave-entry region (Fig. 5(*b*)) and the interaction region (Fig. 5(*c*)). In the wave-entry region only the hardness at the surface reaches the value of R_A60. On the other hand, the hardness profile traced through the center of the transformation triangle shows a gradual hardness decrease. The hardness data show that the isolated shock waves only generated the HCP ϵ phase along a very thin surface layer; this is consistent with the calculations made in Section 3 which show that the expected pressure is of 13 GPa.

Figure 6 shows optical micrographs typical of a region subjected to a pressure below 13 GPa (Fig. 6(*a*)), of a region subjected to a pressure above 13 GPa (Fig. 6(*b*)), and of the interface (Fig. 6(*c*)). Below 13 GPa profuse twinning is induced by the shock wave. This type of substructure is characteristic of shock-loaded steel that was in the annealed condition (*e.g.*, Ref. 14). Although the α (bcc) $\rightarrow \epsilon$ (HCP) transformation is reversible, it is known to leave behind residues that can be clearly seen in the microstructure. The interface between the two regions shown in Fig. 6(*c*) is very clear and well defined.

The dimensions of the transformed regions can be used to obtain information on the shock-wave configuration. The following can be obtained:

a. Rarefaction rate of wave. By making a series of plots similar to the one of Fig. 3(*b*) one can see that the width of the transformed region is equal to the width of the individual pressure pulses at the various depth levels

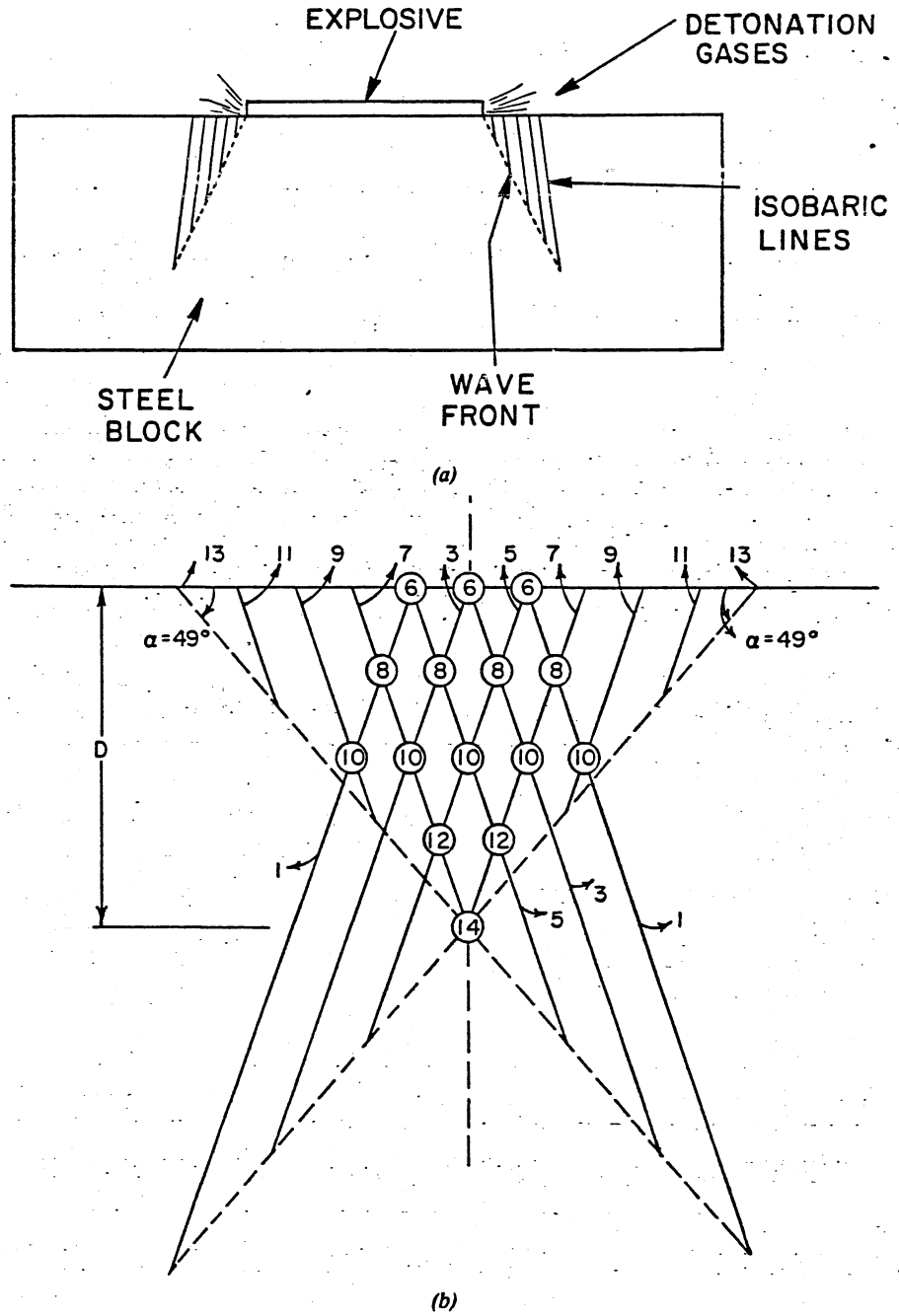

Fig. 3—(*a*) Schematic representation of the converging shock waves. (*b*) Shock-wave configuration during superposition. Total pressures are circled. Full lines are isobars and dashed lines show shock fronts.

D below the surface. One can therefore determine the average rarefaction rates at the surface of the block. Since the individual waves have a pressure of 13 GPa, and the width of the transformed regions at the surface are given in Table I, one obtains rarefaction rates of 3.3, 1.3, and 0.86 GPa/mm for the systems subjected to three, four and five layers of Plastex-P, respectively. It is assumed for simplicity that the rarefaction is linear. These results agree with qualitative statements[4,5] on the effect of the thickness of the explosive layer on the rarefaction rate.

b. Attenuation rate of wave. The depth of the transformed region corresponds to the distance required to attenuate the wave from its initial value to 6.5 GPa, so that the central wave superposition produced 13 GPa. Assuming that this attenuation has a constant rate, it can be calculated by dividing 6.5 GPa by the depth of the transformed region. One obtains attenuation rates of 0.14, 0.13 and 0.12 GPa/mm for the systems subjected to three, four, and five explosive layers, respectively.

Knowing the rarefaction and attenuation rate of a "saw-tooth"-shaped wave it is possible to reconstruct it; this is shown in Fig. 7. The fronts are indicated by dashed lines, while the isobars at 6.5 and 0 GPa show the rarefaction of the wave. It is recognized that several simplifying assumptions were introduced in the reconstruction of the wave. First, four velocity regimes were assumed; from 13 to 10 GPa, the angle α was taken as 49.4 deg; from 10 to 6.5 GPa, it was taken as 48.0; from 6.5 to 3.5 GPa, it was taken as 46.2 deg; and from 3.5 to 0 GPa, it was taken as 44.2 deg. Actually, there is a continuous decrease in the shock-wave velocity with an attendant continuous change in α. Second, it was

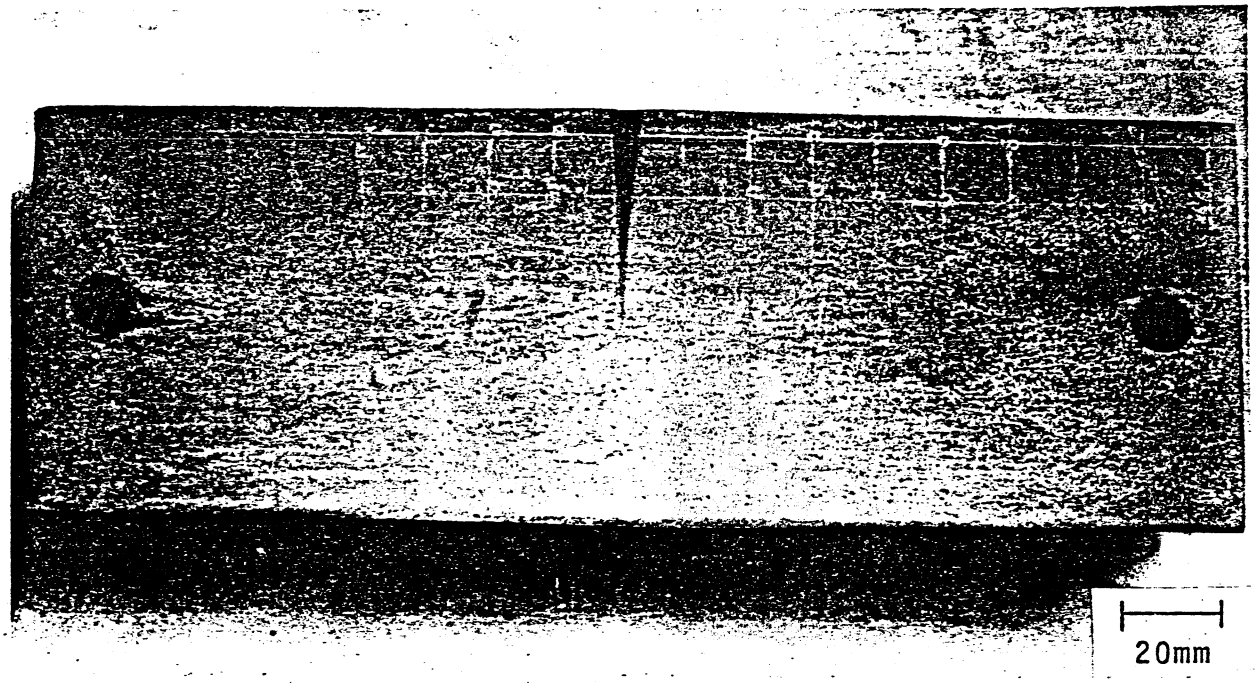

(a)

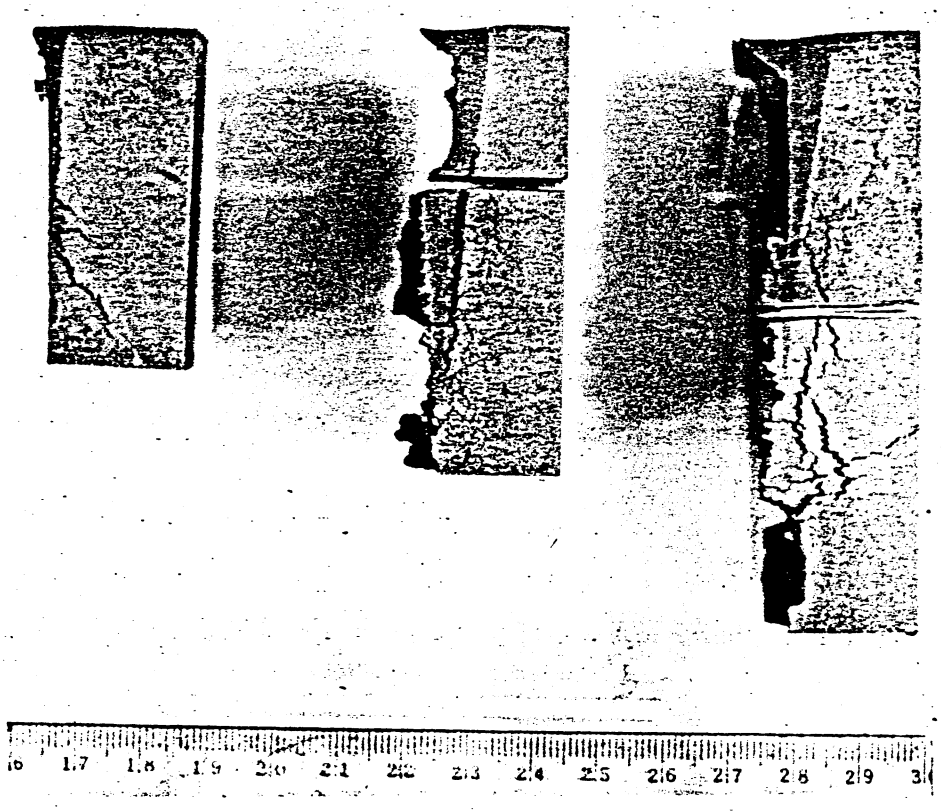

(b)

Fig. 4—(*a*) Macrograph of internal face of block subjected to three explosive layers. (*b*) From left to right, transformation regions in systems subjected to three, four and five Plastex-P layers.

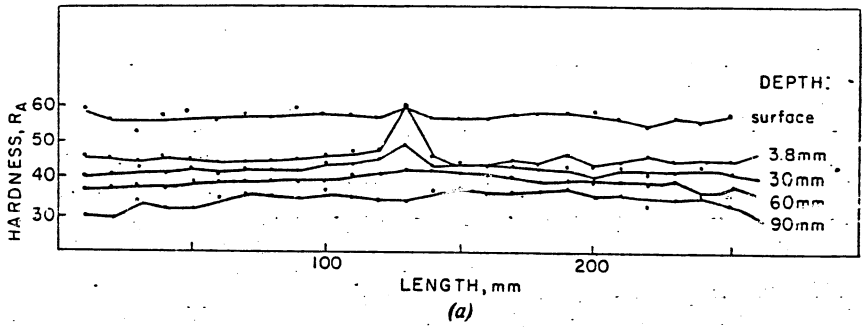

(a)

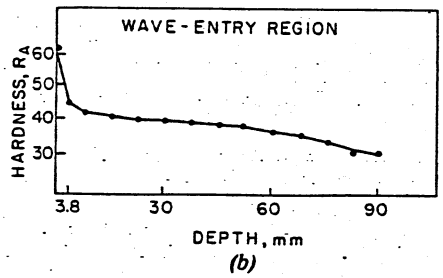

(b)

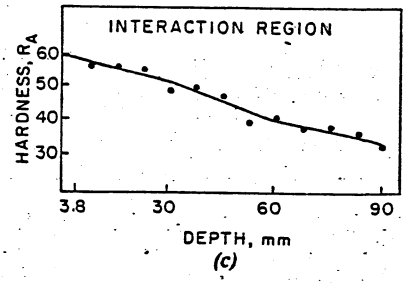

(c)

Fig. 5—Hardness profiles for block subjected to three explosive layers. (*a*) Profiles at surface and parallel to it, at depths of 3.8, 30, 60, and 90 mm below surface. (*b*) Profile along line perpendicular to top surface, at the edge of block (wave-entry region). (*c*) Profile along line perpendicular to top surface, at the wave-superposition region.

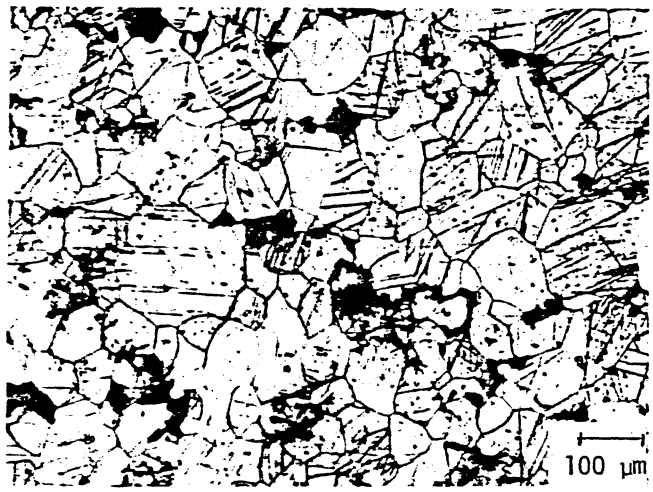

(a)

(c)

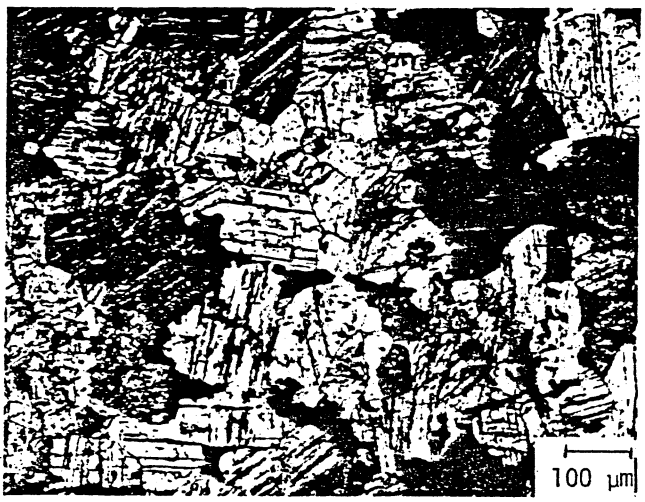

(b)

Fig. 6—Micrographs of system subjected to three explosive layers. (*a*) light region ($P < 13$ GPa), (*b*) dark region ($P > 13$ GPa), (*c*) interaction region.

assumed that the isobars at 6.5 and 0 GPa, on the rarefaction side of the wave were parallel. It can be seen that the increase of the explosive thickness affects the rarefaction rate much more than the attenuation rate.

It is recognized that the technique herein described for determining shock-wave profiles is only an approximate one; much more precise results can be used by modern instrumentation techniques, such as the VISAR[15]. The main advantage of the proposed technique resides in the fact that no instrumentation is needed, rendering the experiments very easy to perform.

4.2 Fracture

The lateral momentum traps could not stop the reflected tensile waves from completely fracturing the systems with four and five Plastex-P layers and from producing an incipient fracture in the system with three

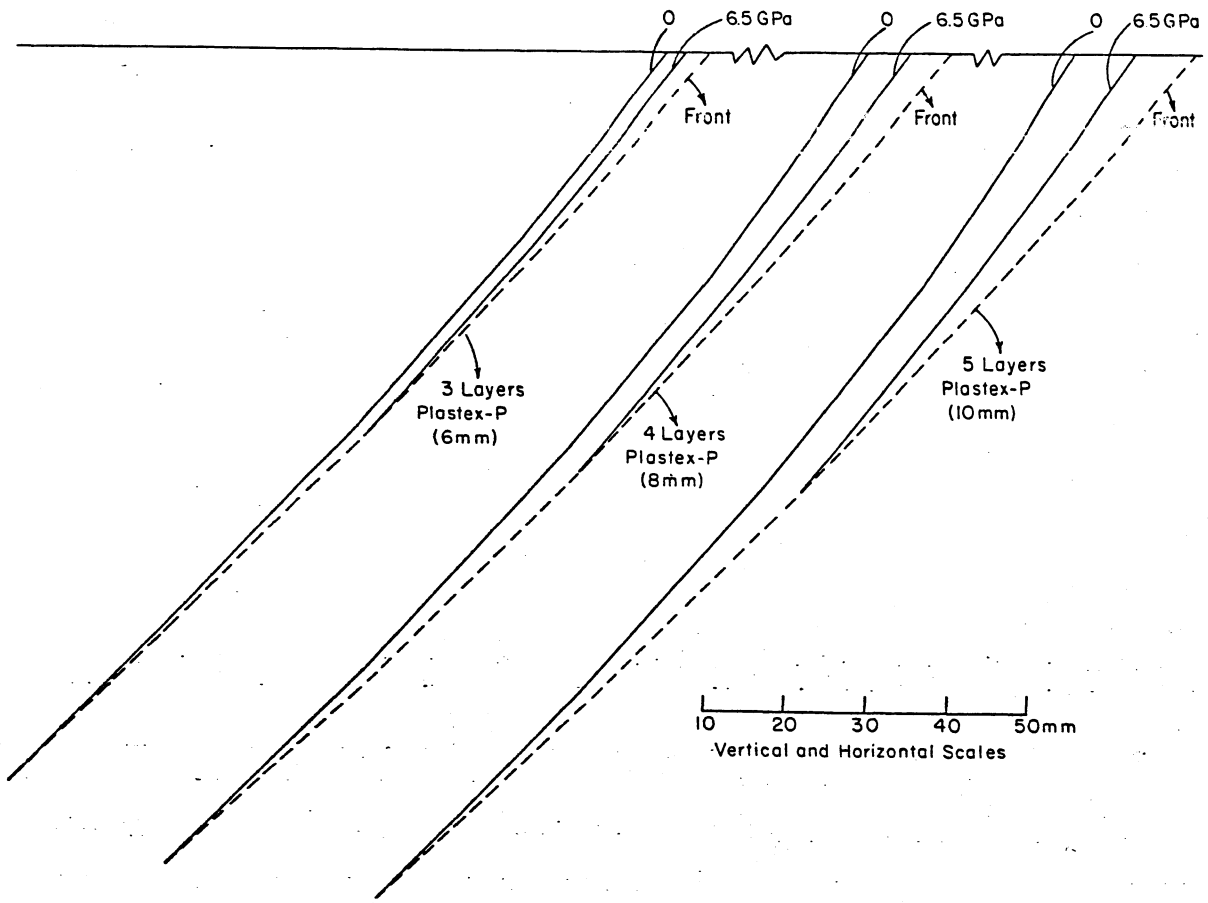

Fig. 7—Estimated shock waves for the three systems.

Table I. Dimensions of Dark Regions

System	Width (mm)	Depth (mm)
3 layers Plastex-P	3.5–5.0	46
4 layers Plastex-P	10	52
5 layers Plastex-P	15	53

layers of Plastex-P. The intensity of the reflected waves was not high enough to produce spalling in the lateral surfaces of the blocks. However, upon returning to the center of the block the reflected tensile waves reinforced themselves upon superimposing, generating fracture in the central region of the block for all three cases. Figure 8 shows the incipient fracture for the 3-layer explosive block. There are two distinct mechanisms operating: a) the fracture with a $\rangle\!\!-\!\!\langle$ shape formed during the passage of the shock waves, and b) the irregular fracture formed by the reflected tensile waves. These two fractures present entirely different morphologies, as can be seen from the scanning-electron fractographs of Fig. 9. The dynamic fracture formed during the passage of the shock waves and due to their interaction is exceptionally smooth, considering that one is dealing with AISI 1020 steel (Fig. 9(*a*)). On the other hand, the fracture produced by the reflected tensile waves is irregular in shape, and exhibits the appearance characteristic of these steels (Fig. 9(*b*)). The smooth spalls have been previously observed by Ivanov and Novikov[16] and Erkman[17] and attributed to the special wave configurations induced by the α (bcc) $\rightarrow \epsilon$ (HCP) polymorphic transformation of iron and steel. Another indication in favor of the existence of two distinct fracture mechanisms is the fact that the smooth spall occurred precisely at the center of the transformed region for the three systems. If the smooth spall had been produced by the reflected tensile waves, it would not occur in precisely the center of the transformed regions, because of the imperfections of the system. In fact, the transformed region for the system subjected to three layers of Plastex-P is at 1 cm from the center of the block. If the smooth spall were due to the reflected waves, their trajectory after intersection indicates that they would intersect again, after reflection, at 2 cm from the transformation region.

The formation of the smooth spall can be understood by the sequence shown in Fig. 10. The spalling is due to the formation of a rarefaction shock generated by the reverse ϵ (hcp) $\rightarrow \alpha$ (bcc) transformation that takes place upon decrease of the overall pressure. The reverse transformation takes place at a lower pressure: 9.8 GPa[18]. Rarefaction shocks were originally postulated by Drummond[19]. The fact that shock waves have to be compressive in nature is dependent on the condition $(\partial^2 P/\partial V^2) > 0$, where P and V are the pressure and volume, respectively. The polymorphic phase transformation produces a "break" in the P-V curve at 13

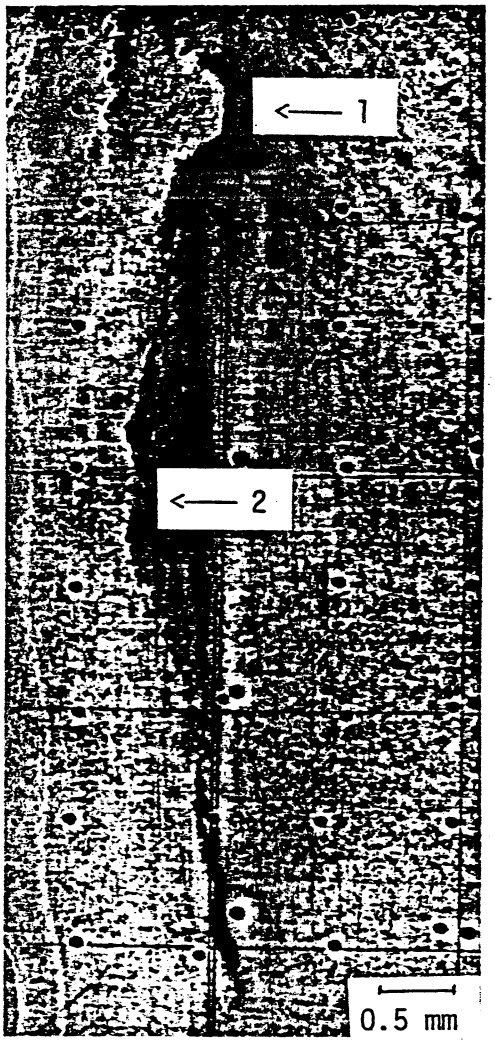

Fig. 8—Incipient fracture for system subjected to three explosive layers. Two mechanisms operate sequentially. First, the smooth spall with a)——(shape is formed (1); then the irregular fracture is formed (2).

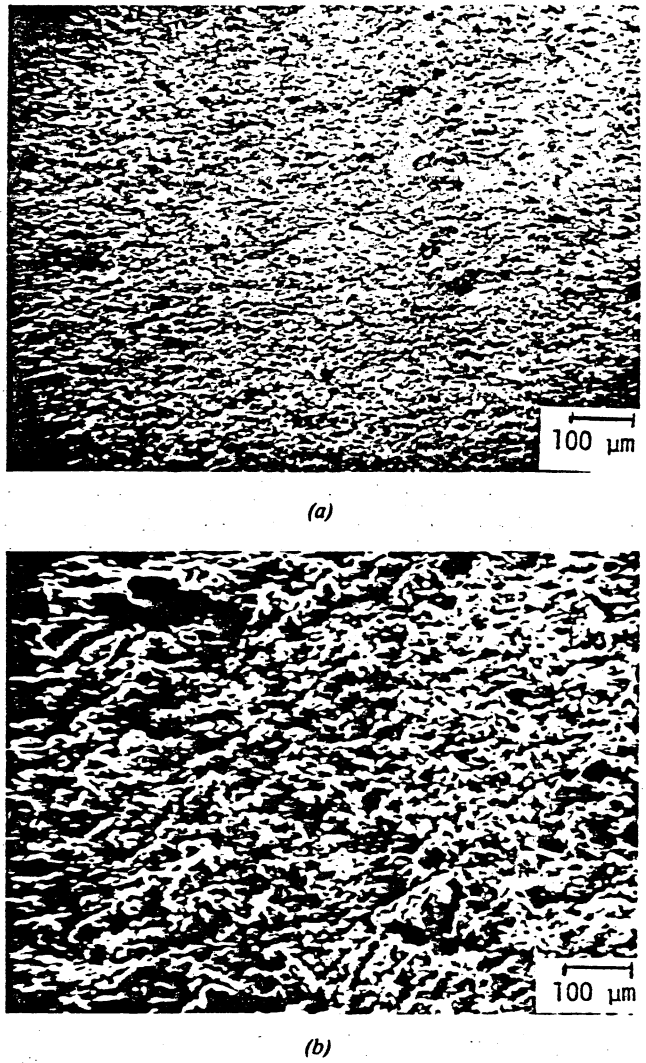

Fig. 9—Scanning-electron micrographs of two fracture regions: (*a*) smooth spall ((1) in Fig. 8), (*b*) irregular spall ((2) in Fig. 8).

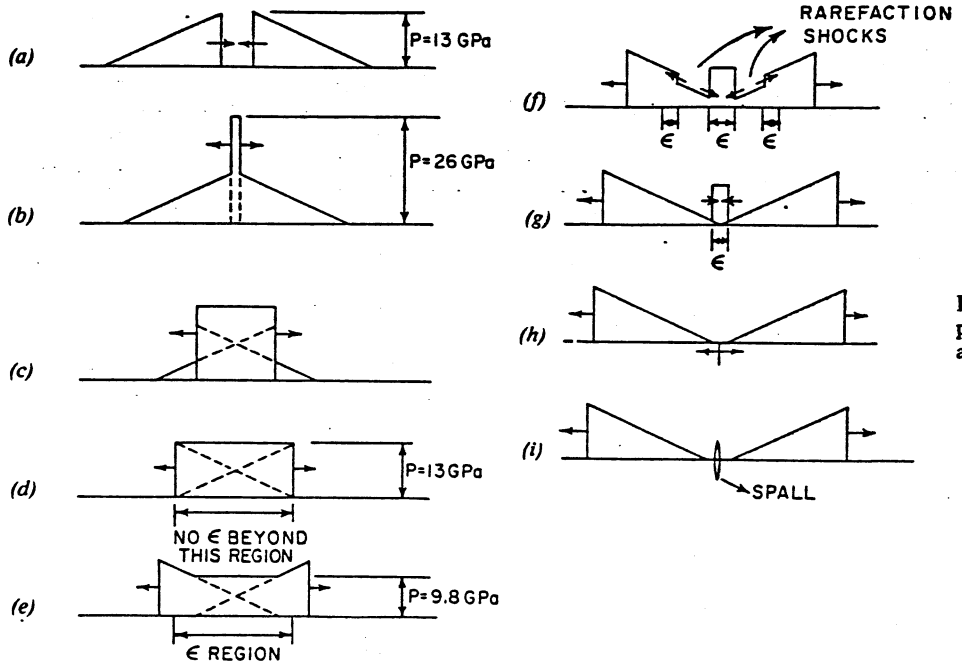

Fig. 10—Sequence of shock wave superposition showing how the interaction shocks and smooth spalling are formed.

GPa, and the above condition is not obeyed making tensile or rarefaction shocks possible. These rarefaction shocks were considered by Erkman[17] and Ivanov and Novikov[16] to be responsible for the smooth spalls. In the present case a similar situation is thought to occur, and shock waves forming in the rarefaction part of the wave are thought to interact and create a sudden high tensile load along a plane, producing the smooth spall. The sequence displayed in Fig. 10 shows how this is accomplished; it shows the pressure pulses at the surface of the block. The incoming waves (*a*) intersect each other, resulting in a rise of the pressure from 13 to 26 GPa (*b*). As the waves progress, the peak pressure decreases (*c*). When the total pressure reaches the value of 13 GPa (*d*) the region of transformation has reached its maximum width. Beyond that point, the ϵ region remains stable until the pressure in the rarefaction plateau reaches the value of 9.8 GPa (*e*). At this point, the ϵ (hcp) $\rightarrow$ α (bcc) reverse transformation is initiated at the rarefaction tail; it propagates into the ϵ region, forming two rarefaction shocks. As the rarefaction shocks converge (*g*) they reduce the extent of the ϵ region. The particle displacements are such that a high tensile stress is established when the two rarefaction shocks intersect; the particle displacements have directions opposite to the shock direction. This tensile stress has very small time rise (the time rise of a shock wave is typically of 10^{-9} s) and the dynamics of fracturing are different from conventional spalling by reflected tensile waves. Consequently the smooth spall results (*i*).

5. CONCLUSIONS

1. A method of obtaining rarefaction and attenuation rates in shock waves produced by contact explosives is described. It uses "internal markers" generated by the polymorphic α (bcc) $\rightarrow$ ϵ (hcp) transformations. The main advantage of the technique is that no instrumentation is required.

2. This method can also be applied to normally incident shock waves generated by explosives or plate impact, by starting the detonation at two opposite parallel faces of a workpiece.

3. It is shown that both the attenuation and rarefaction rates decreased with increasing thickness of the explosive layer. For explosive thicknesses (Plastex-P) of 6, 8, and 10 mm the rarefaction rates of the shock wave at the surface were 3.3, 1.3, and 0.86 GPa/mm, respectively; the attenuation rates were 0.14, 0.13, and 0.12 GPa/mm, respectively. These values are calculated assuming linear rarefaction and attenuation rates.

4. Spalling of the blocks occurred and it is shown that there are two different mechanisms operating: a) a smooth spall is caused by the rarefaction shocks generated during the superposition of the shock waves and due to the reverse transformation ϵ (HCP) $\rightarrow$ α (bcc); b) the shock waves reflect themselves at the ends of the blocks and are not completely trapped by the lateral momentum traps, returning as tensile waves. Upon intersecting they reinforce each other and produce a rough and irregular fracture.

5. The technique could be applied to harden selected regions on the surface of steel blocks.

ACKNOWLEDGMENTS

The last part of this work and the writing of the manuscript were supported by National Science Foundation (Grant DMR79-27102). The cooperation of the following units of the Brazilian Army are gratefully acknowledged: Presidente Vargas Plant, for the development of Plastex-P; Marambaia Proving Ground, for help in the execution of the explosive events; the War Arsenal, for machining the blocks; the Itajubá Weapons Plant, for the heat treatments.

REFERENCES

1. W. C. Leslie: *Metallurgical Effects at High Strain Rates*, R. W. Rohde, B. M. Butcher, J. R. Holland, and C. H. Karnes, eds., Plenum Press, New York, 1973, p. 571.
2. J. S. Rinehart: *Stress Transients in Solids*, Hyperdynamics, Santa Fe, NM, 1975.
3. G. E. Duvall and G. R. Fowles: *High Pressure Physics and Chemistry*, R. S. Bradley, ed., chapt. 9, Academic Press, NY, 1963.
4. O. E. Jones: *Proc. of Behavior and Utilization of Explosives in Engineering Design*, L. Davidson *et al*, ed., p. 125, New Mexico Section, ASME, Albuquerque, NM, 1972.
5. R. N. Orava and R. H. Wittman: *Proc. 5th Internat. Conf. on High Energy-Rate Fabrication*, p. 1.1.1, Denver Research Institute, U. of Denver, Denver, CO, July 1975.
6. S. Katz, D. G. Doran, and D. R. Curran: *J. Appl. Phys.*, 1959, vol. 30, p. 568.
7. L. M. Barker: *J. Appl. Phys.*, 1975, vol. 46, p. 2544.
8. W. E. Drummond: *J. Appl. Phys.*, 1957, vol. 28, p. 1437.
9. W. E. Drummond: *J. Appl. Phys.*, 1958, vol. 29, p. 167.
10. J. E. Erkman: *Phys. of Fluids*, 1958, vol. 1, p. 535.
11. G. E. Dieter: *Response of Metals to High-Velocity Deformation*, P. G. Shewmon and V. F. Zackay, eds., Interscience, New York, 1961, p. 419.
12. E. G. Zukas: *Met. Eng. Q.*, 1966, vol. 6, May, p. 1.
13. G. T. Gray III: M.Sc. Thesis, Department of Metallurgical Engineering, South Dakota School of Mines and Technology, Rapid City, SD, 1977.
14. S. Mahajan: *Phys. Status Solidi*, 1969, vol. 33, p. 291.
15. L. M. Barker and R. E. Hollenbach: *J. Appl. Phys.*, 1972, vol. 43, p. 4669.
16. A. G. Ivanov and S. A. Novikov: *J. Exp. Theor. Phys., (U.S.S.R.)*, 1961, vol. 40, p. 1880.
17. J. O. Erkman: *J. Appl. Phys.*, 1961, vol. 31, p. 939.
18. L. M. Barker and R. E. Hollenbach: *J. Appl. Phys.*, 1974, vol. 45, p. 4872.
19. W. E. Drummond: *J. Appl. Phys.*, 1957, vol. 28, p. 998.